International Journal of Mechanical Engineering (IJME)
ISSN(P): 2319-2240; ISSN(E): 2319-2259
Vol. 5, Issue 4, Jun - Jul 2016; 63-74

International Academy of Science, Engineering and Technology
Connecting Researchers; Nurturing Innovations

COMPUTATIONAL FLUID DYNAMICS ANALYSIS OF IMPELLR DESIGN FOR A PUMP

SURESH PITTALA & DIRIBA T

School of Mechanical & Electro Mechanical Engineering, Hawassa University, Hawassa, Ethiopia

ABSTRACT

The main objective of this present investigation is to design and analyse pump impeller to give better performance than the existing once. Designing impellers are important for fluid flow analysis for a pump. The impeller of an existing industrial pump was analysed and redesigned using an integrated, design/analysis, turbo machinery geometry modelling and flow simulation system. The purpose of the redesign was to achieve improved impeller performance. To improve the efficiency of pump, computational fluid dynamics (CFD) analysis is one which is used in the pump industry. In the present model Acrylonitrile butadiene styrene (ABS) material is used to reduce noise and cutting down the cost of the impeller. The number of impeller blades is proposed to increase from 6-8 to 16 in order to increase fluid velocity. Inlet blade angle is reduced to less than 35 degrees from greater than 55 degrees to increase efficiency and outlet fluid velocity of the impeller. From the CFD analysis to calculate the efficiency of the existing impeller by using the empirical relations. In the first case outlet angle is increased, and in the second case inlet angle is decreased and they are obtained from the CFD analysis.

KEYWORDS: Computational Fluid Dynamics (CFD) Analysis, Impeller Design, Pump

INTRODUCTION

Impellers are prevalent for much different application in the industrial or other sector. Nevertheless, their design and performance prediction process is still a difficult task mainly due to the great number of free geometric parameters, the effect of which cannot be directly evaluated. The significant cost and time of the trial and error process by manufacturing and testing of physical prototype reduces the profit margins of the impeller manufacturers. For this reason CFD analysis is currently used in hydrodynamic design for different impeller types. Impeller is a rotating part of a centrifugal compressor and pump that imparts kinetic energy to a fluid. Here under we introduced (1) modelling laws and (2) Vibration and noise [1, 2].

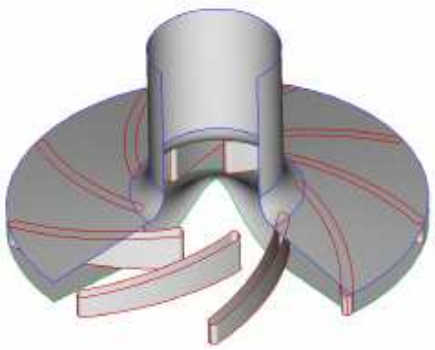

Figure 1: IMPELLER

Modelling Laws The modelling laws includes both the affinity law and model law. These two laws are stated as

follows: **Affinity Law** "for similar conditions of flow the capacity will vary directly with the ratio of speed and/or impeller diameter and the head with the square of this ratio at the point of best efficiency". **Model Law**[3] **"**two geometrically similar pumps working against the same head will have similar flow conditions if they run at speeds inversely proportional to their size, and in that case their capacity will vary with the square of their size". **Vibration and noise** Here we introduce mechanical noise source and methods for reducing noise. **Mechanical noise source** the two comely used mechanical noise source are described as: (a) Common mechanical sources that may produce noise include vibrating pump components or surfaces because of the pressure vibration that are generating in the liquid or air. Example: Impeller or seal rubs, Vibrating pipe walls, unbalanced rotors. (b) In centrifugal machines, improper installation of couplings often causes mechanical vibration at twice pump steep.

Methods for reducing noise the following are the comely used methods for reducing noise inside a mechanical operates. (a) Increase or decrease the pump speed to avoid system resonances of the mechanical system. (b) Decrease suction lift, increase air pressure. (c) Suction pipe should be straight. It is well known [4, 5, 6] that three dimensional flow characteristic for an impeller of an axial turbo fan for improving the airflow rate and the static pressure The pitch angles of 44°, 54°, 59°, and 64° are implemented for the numerical model. The numerical results show that airflow rates of each pitch angle are 1,175

CMH, 1,270 CMH, 1,340 CMH, and 800 CMH, respectively. The difference of the static pressure at impeller inlet and outlet are 120 Pa, 214 Pa, 242 Pa, and 60 Pa according to respective pitch angles. It means that the 59° of the impeller pitch angle is optimal to improve the airflow rate and the static pressure.

Also it is known that [7] the turbo machinery flow is unsteady due to the relative motion between different components of the machine: Furthermore, in hydraulic machines the flow is fully turbulent and three-dimensional. Computing the entire real flow (unsteady and turbulent) through the whole pump requires a large computer memory and computational time even for the most performing computers. Thus, a simplified simulation technique must be used in order to obtain useful results in a storage pump.

Secondary flows are undesirable in centrifugal pumps as they are a direct cause for flow (head) losses, create non uniform meridional flow profiles, potentially induce flow separation/stall, and contribute to impeller flow slip; that is, secondary flows negatively affect the compressor performance [8]. A model based on the vorticity equation for a rotating system was developed to determine the stream wise vorticity from the normal and bi-normal vorticity components, which are known from the meridional flow profile. Using the stream wise vorticity results and the small shear-large disturbance flow method, the onset, direction, and Magnitude of circulatory secondary flows in a shrouded centrifugal impeller can be predicted. This model is also used to estimate head losses due to secondary flows in a centrifugal flow impeller. The described method can be employed early in the design process to develop impeller flow shapes that intrinsically reduce secondary flows rather than using disruptive elements such as splitter vanes to accomplish this task.

The performance and flow structure in an unshrouded impeller of approximately 4:1 pressure ratio is synthesized on the basis of a detailed analysis of 3D viscous CFD results and aerodynamic measurements [9]. A good data match was obtained between CFD and measurements using laser anemometry and pneumatic probes.

Results are presented showing the loss production and secondary flow structure in the Impeller. The results indicate that while the overall impeller efficiency is high, the impeller shroud static pressure recovery potential is

underdeveloped leading to performance degradation in the downstream diffusing element. Thus, a case is made for a follow on impeller parametric design study to improve the flow quality. A strategy for aerodynamic performance enhancement is outlined and an estimate of the gaining overall impeller efficiency that might be realized through improvements to the relative diffusion processes provided.

A finite element based method has been developed [10] for computing fluid- induced forces on an impeller in a volute casing. Potential flow theory is used assuming irrigational, in viscid and incompressible flow. Both excitation forces and motion dependent forces are calculated. The numerical results are compared with experimental results obtained at the California Institute of Technology. In two-dimensional and three-dimensional simulations the calculated pump characteristics near the design point are about 20% higher than the experimental curve. This is caused by viscous losses that are not taken into account in our model. The magnitude of the excitation force is predicted well for optimum and high flow rates. At low flow rates the calculated force is too large which is probably related to inaccuracies in the calculated pressure.

Computational Fluid Dynamics (CFD)

As the phrase indicates, ***computational fluid dynamics*** encompasses two disciplines, computation and fluid dynamics. Together, these disciplines are used to numerically simulate the real fluid dynamics through modelling. The CFD technology is critical in efforts to lower the development costs and to improve and extend the performance and effectiveness of flight vehicles, of air breathing engines, of ocean vehicles, of parachutes, and of manufacturing processes involving fluid flows.

This technology is necessary for operating wind tunnel test facilities more efficiently and for enhancing flight-tests operations and flight safety during flight vehicle development programs. Furthermore, this technology can revolutionize the design and analysis processes, when fluid dynamics is coupled with other disciplines such as electromagnetic, optics, structures, and flight dynamics.

CFD is one of the branches of fluid mechanics that uses numerical methods and algorithms to solve and analyse problems that involve fluid flows. Computers are used to perform the millions of calculations required to simulate the interaction of fluids and gases with the complex surfaces used in engineering. Even with simplified equations and high-speed supercomputers, only approximate solutions can be achieved in many cases. On-going research, however, may yield software that improves the accuracy and speed of complex simulation scenarios such as transonic or turbulent flows. Initial validation of such software is often performed using a wind tunnel with the final validation coming in flight test.

CFD is used in design and analysis under the following conditions. The design specifications of a fluid dynamics system are essentially determined by the Performance quantities and, to some extent, by the global flow fields. The performance estimates are required for predicting the operational performance of the system, making design evaluations, determining design sensitivities and optimization, and establishing a design data base. Increments in performance estimates are required for design trade off studies. The global flow fields are useful for understanding the fluid dynamics and also for making trade off studies. Often, results based on complex CFD methods are used to develop or calibrate simple methods. Furthermore, computations enhance the credibility and usefulness of ground-based and flight tests conducted for design and analysis, and they reduce costs for conducting these tests. Prefabrication (that is, before a test model is fabricated) computations can provide a sanity check of the proposed test program.

Fluid dynamics is a field of science which studies the physical laws governing the flow of fluids under various conditions. Great effort has gone into understanding the governing laws and the nature of fluids themselves, resulting in a complex yet theoretically strong field of research.

The Physical aspects of any fluid flow are governed by three fundamental principles Mass is conserved; Newton's second law and Energy is conserved. These fundamental principles can be expressed in terms of mathematical equations, which in their most general form are usually partial differential equations. CFD is the science of determining a numerical solution to the governing equations of fluid flow whilst advancing the solution through space or time to obtain a numerical description of the complete flow field of interest.

The result of CFD analyses is relevant engineering data used in (a) Conceptual studies of new designs (b) detailed product development (c) trouble shooting, redesign.

The Mathematics of CFD

The set of equations which describe the processes of momentum, heat and fluid flow are known as the Navier-Stokes equations. These partial differential equations were derived in the early nineteenth century and have no known general analytical solution but can be discredited and solved numerically. Equations describing other processes, such as combustion, can also be solved in conjunction with the Navier-Stokes equations.

Often, an approximating model is used to derive these additional equations, turbulence models being a particularly important example.

Methods and Governing Equations

CFD solvers are usually based on the finite volume method that includes the following steps: (a) Domain is discredited into a finite set of control volumes or cells. (b) General conservation or transport equation for mass, momentum, energy, etc., are discredited into algebraic equations which are shown in figure 2. (c) All equations are solved to render flow field.

Analysis begins with a mathematical model of a physical problem that includes the following steps: (a) Conservation of matter, momentum, and energy must be satisfied throughout the region of interest. (b) Fluid properties are modelled empirically. (c) Simplifying assumptions are made in order to make the problem track able (e.g., steady-state, incompressible, in viscid, two-dimensional. (d) Provide appropriate initial and/or boundary conditions for the problem. (e) Governing differential equations become algebraic. (f) The collection of cells is called the grid or mesh. (g) System of equations is solved simultaneously to provide solutions.

CFD applies numerical methods called discretization to develop approximations of the governing equations of fluid mechanics and the fluid region to be studied. The set of approximating equations are solved numerically for the flow field variables at each node.

$$\frac{\partial}{\partial t}\int_v \rho\ \emptyset dv + \oint_A \rho \emptyset V\ .dA\ =\ \oint_A \Gamma\ \nabla \emptyset\ .dA + \int_V s_\emptyset\ dV$$

<Unsteady> + <Convention> = <Diffusion> + <Generation>

Figure 2: General Conversation

CFD Procedure and Analysis

Fluid flow analysis performed on the impeller, using ansys CFX. Numerical results fully characterized the flow field, providing detailed flow information such as flow speed, flow angle, pressure, boundary layer development, losses. The flow field information from CFD simulation was then used to help elucidate the flow physics [12, 13].

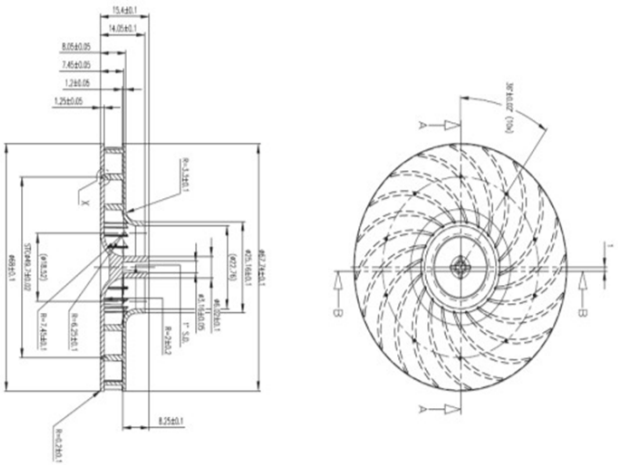

Figure 3: Impeller Geometry Front View and Side View

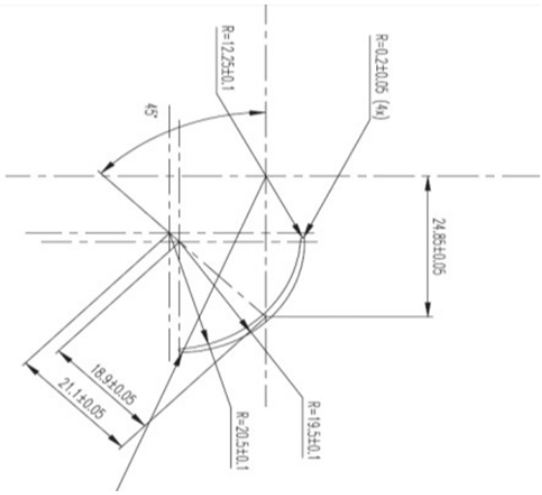

Figure 4: Blade Geometry

Table 1: Design Specification of Impeller

S. No.	Parameter	Size
1.	Inlet diameter (Di)	2 X 22.67 mm
2.	Outlet diameter(D0)	2 X 67.74 mm
3.	Blade number	16
4.	Inlet angle (α)	38o
5.	Outlet angle (β)	620
6.	Blade thickness (t)	2.5 mm
7.	Shaft diameter (Ds)	2 X 6 mm

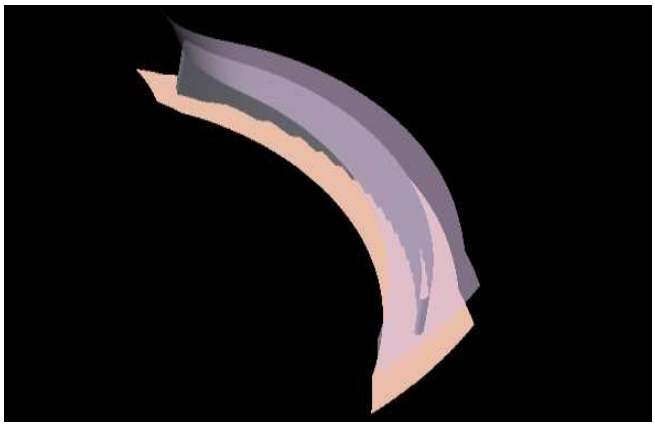

Figure 5: Hub, Shroud and Blade Profiles of an Impeller

Figure 6: Trailing Edge

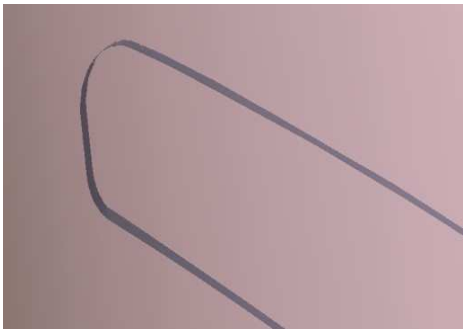

Figure7: Leading Edge

Meshing

Turbo grid uses unstructured meshes in order to reduce the amount of time spent generating meshes, simplifying the geometry modeling and mesh generation process, model more complex geometries than can be handled with conventional, multi-block structured meshes, and let the mesh to be adapted to resolve the flow-field features. This flexibility allows picking mesh topologies that are best suited for particular application. All types of meshes can be adapted in Ansys CFX in order to resolve large gradients in the flow field, but the initial mesh (whatever the element types used) outside of the solver, using Ansys work bench, T Grid, or one of the CAD systems for which mesh import filters exist must always be generated. The geometry is created by using Solid Works and the extruded geometry is meshed by Turbo Grid.

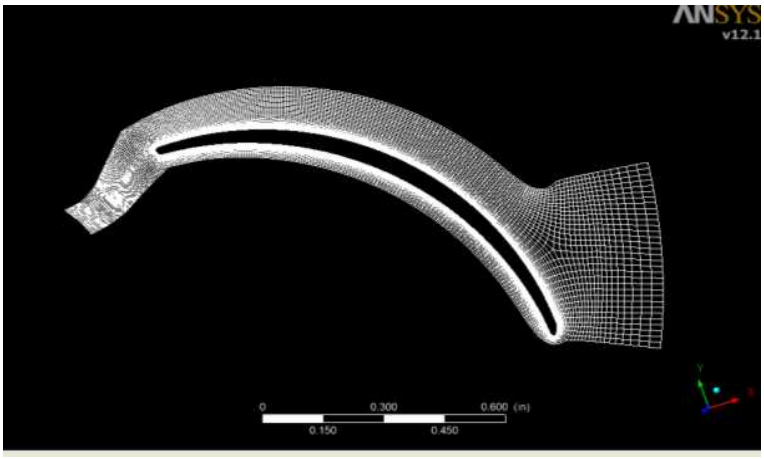

Figure 8: Meshing of Single Blade

Table 2: Mesh Statistics

S. No.	Mesh Measure	Value	% Bed
1.	Minimum face angle	26.2748	0
2.	Maximum face angle	153.725	0
3.	Maximum element	382,072	1.9669
4.	Minimum volume	1,74683e-012 [inches]	0
5.	Maximum edge	1970.8	9.8659

Table 3: Compression between Classical Model and New Model

S. No.	Parameter	Classical Model	New Model	Benefits of New Model
1.	Inlet angle	550	380	Flow increment
2.	Outlet angle	750	620	Flow increment
3.	Number of blades	6	16	Flow increment
4.	Material	Steel	ABS (C8H8)	Cost reduction
5.	Outlet velocity	9.22 m/s	19.46 m/s	Outlet velocity increment

CFX Preprocessor

In the present work, the effect of inflow/outflow boundary conditions on the impeller is studied. Two types of inflow/outflow conditions are considered, static inflow with extrapolated outflow boundary condition 1(BC1), and dynamic inflow boundary condition 2 (BC2) that accounts for upstream influence in the subsonic flow. For the first set of inflow/ outflow boundary condition, uniform flow is specified at the inflow boundary, and all the flow variables at the outflow boundary are extrapolated. For the current problem air as ideal gas has been chosen these have the following properties.

Table 4: Values of Fluid

Molar mass	38.96 kg/kmol
Density	1.024 kg/m^3

RESULTS AND DISCUSSIONS

Static Pressure contours at 10000 rpm at 70 % are shown in the following figure:

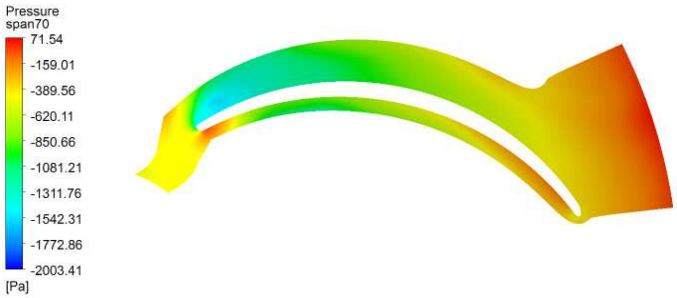

Figure 9: 10000 rpm

From figure 9 the pressure at inlet is as compared to the pressure at outlet in 10000 rpm case but in the 2000 rpm case the pressure at inlet is low and the pressure at outlet is high that means the exit velocity in 2000 rpm is low as compared to 10000 rpm.

Total Pressure contours at 10000 rpm at 70 % are shown in the fooling figures:

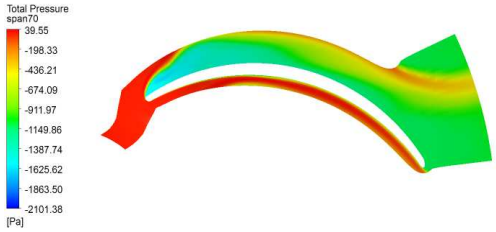

Figure 10: 10000 rpm

Profiles of span wise velocity component are shown in Figures for 10000 rpm respectively. The figures X axis represents axial chord and Y axis represents velocity in m/s. the figures represents flow variations in 10000 rpm at contours 20%, 50%, 70% span wise.

Span Wise Velocity Contours at 10000 rpm at 20 %

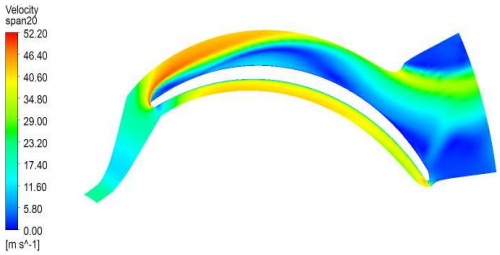

Figure 11: Velocity Contour 20% at 10000 rpm

Mean Span Wise Pressure Profiles

Mean contours of span wise pressure component are shown in Figures for 10000 rpm, 8000 rpm respectively. The figures X axis represents axial chord and Y axis represents pressure in Pa. the figures represents flow variations in 10000 rpm, 8000 rpm at contours 20%, 50%, 70% span wise.

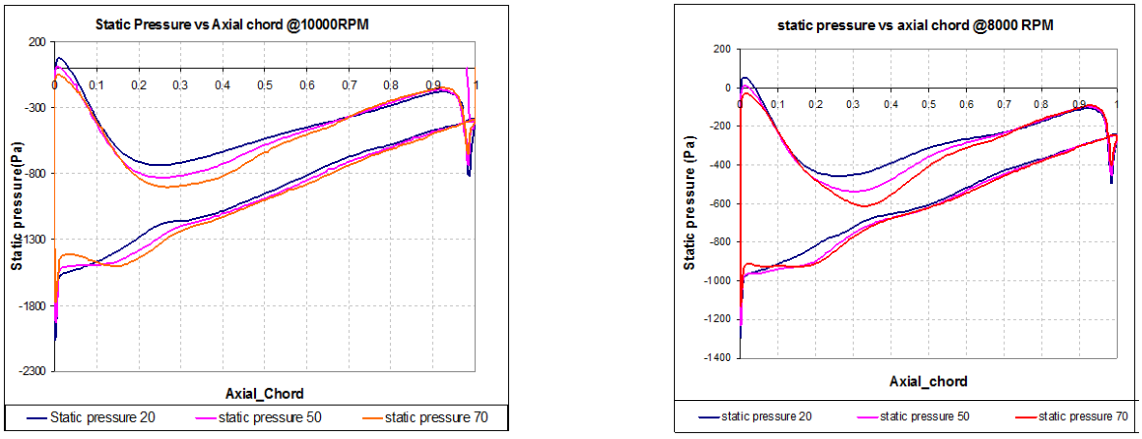

Figure 12: Static Pressure Contours at 20%, 50% and 70% at 10000 rpm and 8000 rpm

Mean Span Wise Total Pressure Profiles

Mean contours of span wise total pressure component are shown in Figures for 10000 rpm, 8000 rpm respectively. The figures X axis represents axial chord and Y axis represents total pressure in Pa. the figures represents flow variations in 10000 rpm, 8000 rpm at contours 20%, 50%, 70% span wise at outlet.

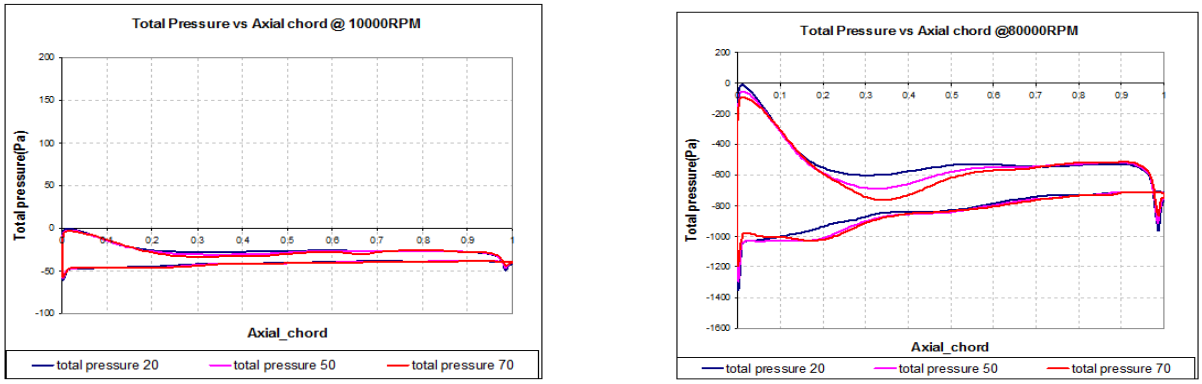

Figure 13: Total Pressure Contours at 20%, 50% and 70% at 10000 rpm and 8000 rpm

Span Wise Velocity Profiles of span wise velocity component are shown in Figures for 10000 rpm, 8000 rpm respectively. The figures X axis represents axial chord and Y axis represents velocity in m/s. the figures represents flow variations in 10000 rpm, 8000 rpm at contours 20%, 50%, 70% span wise

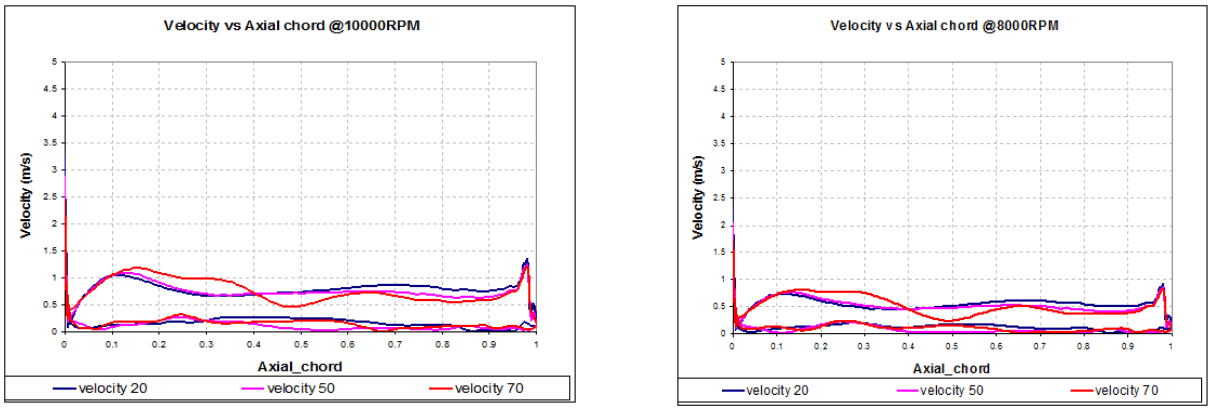

Figure 14: Velocity Contours at 20%, 50% and 70% at 10000 rpm and 8000 rpm

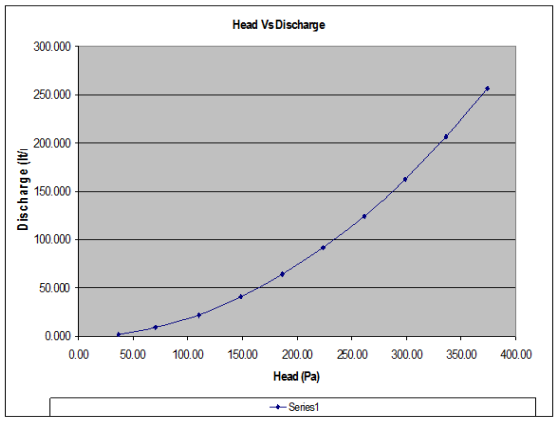

Figure 15: Head vs Discharge

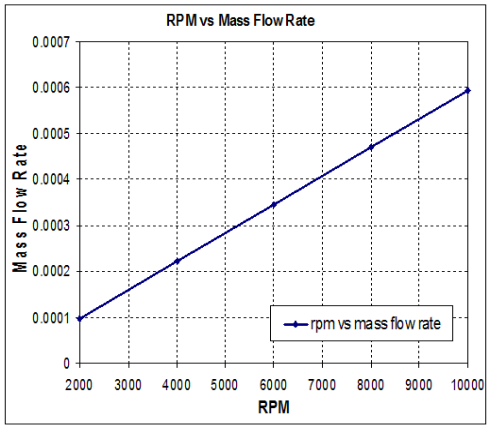

Figure 16: Rpm vs Mass Flow Rate

The graph shows head vs discharge-axis represents head in Pa and Y-axis represents discharge in m3 /s. The above graph shows there is no formation of surge and stall.

RPM vs Mass Flow Rate

The graph (Figure 16) shows at different rpms (10000, 8000, 6000, 4000 and 2000) the behaviour of fluid flow at outlet. If the rpm increases the flow at outlet will also increases. From the figure X-axis represents rpm and Y-axis represents mass flow rate in kg/s.

CONCLUSIONS AND SCOPE

The proposed improvements include (a) Impeller & blade material to be changed (b) Number of blade increases (c) Blade inlet angle to be changed (d) Blade outlet angle to be changed (e) CFD software results compare with the classical and new model.

Analysis was carried out for CFD cases for RPM of 10000, 8000, 6000,

4000 and 2000 It has been observed that all the cases are free from surge and stall. Velocity obtained from the CFD predictions of 19.46 m/s is achieved at outlet for the 10000 rpm case. There is no formation of wake in any of the cases. It has been observed that velocity of the fluid is directly proportional to impeller's RPM. Correlation has been derived between Head and Discharge. Correlation has been derived between RPM and Mass flow rate.

REFERENCES

1. Labanoff Robert R. Ross, Centrifugal blower impeller design & application Gulf Publishing Company, Houston, TX, 1992, volume-2.
2. T.E.Stirling : "Analysis of the design of two pumps using NEL methods" Centrifugal Pumps-Hydraulic Design-I Mech E Conference Publications 1982-11, C/183/82.
3. Numerical Calculation of the flow in a centrifugal blower impeller using Cartesiangrid procedure of 2nd WSEAS int.Conference on applied and theoretical mechanics, Venice, Italy, November20-22,2006,According to john S.Anagnostopoulos.
4. Young-Kyun Kim, Tae-Gu Lee, Jin-Huek Hur, Sung-Jae Moon, and Jae-Heon Lee World Academy of Science, Engineering and Technology 50 2009.
5. International Journal of Rotating Machinery 2005:1, 45–522005 Hindawi Publishing Corporation Mechanical and Fluids Engineering Department, Southwest Research Institute, 6220 Culebra Road, an Antonio, TX 78238-5166, USA.
6. MA Xi-jin, ZHANG Huachuan, ZHANG Kewei. Numerical Simulation and Experiment Analysis of Thirdly Circulating Feed-water Mixed-flow Pump in Nuclear Power Station. FLUID MACHINERY. Vol.37, No.09, 2009 6-9.
7. Georgiana DUNCA1, Sebastian MUNTEAN 2, Eugen Constantin ISBĂŞOIU3, U.P.B. Sci. Bull., Series D, Vol. 72, Iss. 1, 2010.
8. Miner S.M. 2001, 3-D viscous flow analysis of a mixed flow pump impeller, International Journal of Rotating Machinery, Vol. 7, No. l, pp. 53-63.

9. Prepared for the33rd Joint Propulsion Conference and Exhibit cosponsored by AIAA, ASME, SAE, and ASEESeattle, Washington, July 6–9, 1997.
10. The 1997 ASME Fluids Engineering Division Summer Meeting FEDSM'97, June 22–26, 1997.
11. Yun Chuan-yuan. Numerical Calculation of Turbulent Flow, Performance Experiment Mixed-flow Pump Impeller. Transactions of the Chinese Society for Agricultural Machinery. V01.39, No.3 2008. 52-55.
12. JIA Rui-xuan, XU Hong. Optimal design of low specific speed mixed-flow pumps impeller. Journal of Drainage Irrigation Machinery Engineering. Vol. No.02, 2010, 98-102.
13. S. Cao, G. Peng, and Z. Yu, Hydrodynamic design of rot dynamic pump impeller for Multiphase pumping by combined approach of inverse design and CFD analysis, ASME Transactions, Journal of Fluids Engineering,Vol.127, 2005, pp. 330-338.